

Reactivity of Bromine Radical with Dissolved Organic Matter Moieties and Monochloramine: Effect on Bromate Formation during Ozonation

Sungeun Lim, Benjamin Barrios, Daisuke Minakata, and Urs von Gunten*



Cite This: *Environ. Sci. Technol.* 2023, 57, 18658–18667



Read Online

ACCESS |

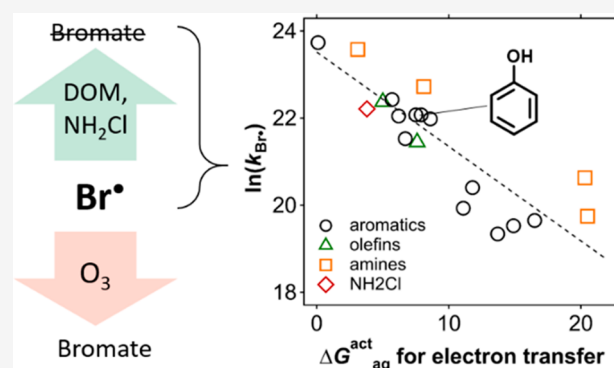
Metrics & More

Article Recommendations

Supporting Information

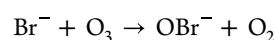
ABSTRACT: Bromine radical (Br^\bullet) has been hypothesized to be a key intermediate of bromate formation during ozonation. Once formed, Br^\bullet further reacts with ozone to eventually form bromate. However, this reaction competes with the reaction of Br^\bullet with dissolved organic matter (DOM), of which reactivity and reaction mechanisms are less studied to date. To fill this gap, this study determined the second-order rate constant (k) of the reactions of selected organic model compounds, a DOM isolate, and monochloramine (NH_2Cl) with Br^\bullet using γ -radiolysis. The k_{Br^\bullet} of all model compounds were high ($k_{\text{Br}^\bullet} > 10^8 \text{ M}^{-1} \text{ s}^{-1}$) and well correlated with quantum-chemically computed free energies of activation, indicating a selectivity of Br^\bullet toward electron-rich compounds, governed by electron transfer. The reaction of phenol (a representative DOM moiety) with Br^\bullet yielded *p*-benzoquinone as a major product with a yield of 59% per consumed phenol, suggesting an electron transfer mechanism. Finally, the potential of NH_2Cl to quench Br^\bullet was tested based on the fast reaction ($k_{\text{Br}^\bullet, \text{NH}_2\text{Cl}} = 4.4 \times 10^9 \text{ M}^{-1} \text{ s}^{-1}$, this study), resulting in reduced bromate formation of up to 77% during ozonation of bromide-containing lake water. Overall, our study demonstrated that Br^\bullet quenching by NH_2Cl can substantially suppress bromate formation, especially in waters containing low DOC concentrations (1–2 mgC/L).

KEYWORDS: bromine radical, bromate, dissolved organic matter, model compounds, reaction kinetics, ozone

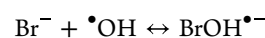


1. INTRODUCTION

Bromide is ubiquitously present in fresh waters in 10–1000 $\mu\text{g/L}$ ^{1,2} and plays an important role in most oxidative water treatment processes.³ During oxidation processes, bromide is converted to reactive bromine species such as hypobromous acid (HOBr^4 and/or bromine(-containing) radicals (e.g., Br^\bullet , $\text{Br}_2^{\bullet-}$, BrO^\bullet).^{5–7} HOBr reacts with dissolved organic matter (DOM) to produce potentially harmful brominated disinfection byproducts (Br-DBPs).^{8,9} Bromine radicals can influence micropollutant abatement^{5,10–12} and algal toxin degradation.^{13,14} A special feature of ozonation is the oxidation of bromide to bromate,¹⁵ which is a probable human carcinogen with a drinking water standard of 10 $\mu\text{g/L}$.^{16,17} Its formation mechanism during ozonation has received considerable research efforts for decades.¹⁸ It is formed by a complex interplay between ozone, hydroxyl radical ($\bullet\text{OH}$), and various reactive bromine species,¹⁸ characterized by two initial pathways: oxidation of bromide (a) to hypobromite (OBr^-) by ozone (eq 1)^{19,20} or (b) to Br^\bullet by $\bullet\text{OH}$ (eqs 2 and 3).^{21,22} The primary products, OBr^-/HOBr and Br^\bullet , serve as key intermediates by subsequently reacting with ozone or $\bullet\text{OH}$ to ultimately form bromate.^{7,18}

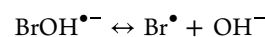


$$k_1 = 1.6 \times 10^2 \text{ or } 2.6 \times 10^2 \text{ M}^{-1} \text{ s}^{-1} \quad (1)$$



$$k_{+2} = 1.1 \times 10^{10} \text{ M}^{-1} \text{ s}^{-1}$$

$$k_{-2} = 3.3 \times 10^7 \text{ s}^{-1} \quad (2)$$



$$k_{+3} = 4.2 \times 10^6 \text{ s}^{-1}$$

$$k_{-3} = 1.3 \times 10^{10} \text{ M}^{-1} \text{ s}^{-1} \quad (3)$$

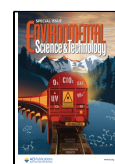
Special Issue: Oxidative Water Treatment: The Track Ahead

Received: October 19, 2022

Revised: December 29, 2022

Accepted: December 29, 2022

Published: January 27, 2023



However, the subsequent reactions to bromate can be interrupted by DOM. HOBr reacts partially with residual electron-rich moieties of DOM, which remain after ozone attack, with second-order rate constants (k) ranging from 10^3 to 10^7 $M^{-1} s^{-1}$.⁴ Likewise, Br^\bullet can react fast with DOM moieties with k_{Br^\bullet} of 10^4 to 10^8 $M^{-1} s^{-1}$.^{23–25} Recently, k_{Br^\bullet} of standard DOM were measured in a range of $(0.5–4.2) \times 10^8$ $M_c^{-1} s^{-1}$.²⁶ During ozonation, the Br^\bullet reaction with DOM is in competition to ozone with $k_{Br^\bullet, O_3} \approx 1.5 \times 10^8$ $M^{-1} s^{-1}$.⁷ A wide range of k_{Br^\bullet} has been reported for micropollutants (10^8 – 10^{11} $M^{-1} s^{-1}$),¹⁰ which implies selectivity of Br^\bullet to organic compounds. Nevertheless, a systematic investigation on the Br^\bullet reactivity with organic moieties including quantitative structure–activity relationship (QSAR) is lacking to date.

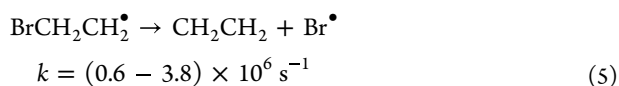
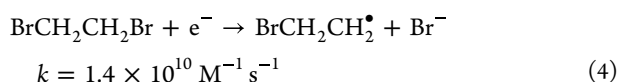
Among diverse bromate mitigation strategies, a sequential addition of chlorine and ammonia prior to ozonation has shown good performance.¹⁸ Direct addition of monochloramine (NH_2Cl) prior to ozonation was also effective to reduce bromate,^{27,28} but questions remain about the underlying mechanism. NH_2Cl was suggested to mitigate bromate by reacting with $\bullet OH$, HOBr, or bromide.^{27,28} However, such reactions are either insufficient to account for a substantial mitigation²⁹ or too slow.³⁰

This study aims to understand the role of Br^\bullet in bromate formation during ozonation, especially with regard to its reactions with DOM and NH_2Cl , with the specific objectives to (1) determine the k_{Br^\bullet} of organic model compounds for DOM and establish QSAR, (2) identify products formed during the reaction of phenol (a representative DOM moiety) with Br^\bullet and elucidate the underlying reaction mechanisms, and (3) investigate the effect of quenching Br^\bullet by NH_2Cl and DOM on bromate formation during ozonation of bromide-containing water.

2. MATERIALS AND METHODS

2.1. Reagents. Details for chemicals and Lake Zurich water composition are provided in Text S1 (Supporting Information). Preparation of DOM and chloride-free NH_2Cl stock solutions is described in Text S2 and Text S3, respectively.

2.2. γ -Radiolysis. γ -radiolysis was carried out by a ^{60}Co γ -radiation source (Gammacell 220, Atomic Energy of Canada, Ltd.) with a dose rate of 0.13 kGy/h (yielding a Br^\bullet formation rate of 9.7 nM/s) determined by a dosimetry in a formate solution (Text S4).⁷ Br^\bullet was formed by the reaction of 1,2-dibromoethane with e^- , according to eqs 4 and 5.^{23,25,31,32}



Samples for determining k_{Br^\bullet} of the organic model compounds were prepared as described in Text S5 and Figure S4. Briefly, mixed solutions containing 3.4 μM ibuprofen (as a competitor), 3.4 μM of a model compound, 0.7 mM 1,2-dibromoethane (for generating Br^\bullet), 4 mM *t*-butanol (for scavenging $\bullet OH$), 50 mM buffer (phosphate for pH 7.1 or borate for pH 10.2), and ~ 50 μM dissolved O_2 (for scavenging C-centered radicals (Text S6)) were prepared and subjected to γ -radiolysis for 0–20 min. Before and during γ -radiolysis, silver nitrate solution was added for masking bromide which is

formed from the reaction of 1,2-dibromomethane with solvated electrons (Text S7). The scavenging rates of the reactive species (e.g., e^- , $\bullet OH$, Br^\bullet) in the applied γ -radiolysis condition were estimated based on kinetic information, as shown in Table S10. After a predetermined time point, the sample was taken out from the γ -radiation source and sodium chloride was added to precipitate residual Ag^+ as AgCl. Samples for identifying products for the reaction of phenol with Br^\bullet were prepared as described in Text S9. Solutions in these vials contained 22 μM phenol, 0.7 mM 1,2-dibromoethane, 40 mM *t*-butanol, and 50 mM phosphate buffer (pH 7.1).

2.3. Competition Kinetics. k_{Br^\bullet} of organic model compounds were determined by competition kinetics with ibuprofen as a competitor based on eq 6 where M and C indicate an organic model compound and a competitor (ibuprofen), respectively. k_{Br^\bullet} of ibuprofen was 3.8×10^9 $M^{-1} s^{-1}$ (see section 3.1.1).

$$\ln\left(\frac{[M]}{[M]_0}\right) = \ln\left(\frac{[C]}{[C]_0}\right) \frac{k_{Br^\bullet, M}}{k_{Br^\bullet, C}} \quad (6)$$

k_{Br^\bullet} for DOM and NH_2Cl was determined by measuring the change in ibuprofen concentration over γ -radiolysis time, by applying varying concentration ratios of ibuprofen (1 μM) and DOM (2–15 mgC/L) or NH_2Cl (0.01–0.4 mM). Details to derive k_{Br^\bullet} under this adapted method are provided in Text S8. All competition kinetics plots are provided in Figures S5 and S6.

2.4. Analyses. High-performance liquid chromatography coupled with a diode array or fluorescence detector (HPLC) and LC coupled with high-resolution tandem mass spectrometry (LC-HRMS/MS) were used for analyzing organic compounds. Reference standards were compared for identified products during the phenol- Br^\bullet reaction. For suspected products by LC-HRMS/MS, the confidence level system (level 1 to 5 with level 5 as the lowest level providing only an exact mass)³³ was used to categorize the MS results. Ion chromatography coupled with a conductivity detector (IC) was used for analyzing chloride and bromate (Text S10).

2.5. Ozonation. Ozone stock solutions were prepared and standardized as described in Text S11. For ozonation experiments, filtered Lake Zurich water was spiked with 2 μM bromide, 1 mM phosphate buffer (pH 7.6), and 5 μM *p*-chlorobenzoic acid (*p*CBA), as mixed concentrations. Additionally, either 10 μM formate, or 4 μM ammonium, or 7 μM NH_2Cl , or 15 μM NH_2Cl was added to the spiked Lake Zurich water to assess different quenching scenarios. An aliquot of the ozone stock solution (ozone dose 60 μM) was added to the Lake Zurich waters to initiate ozonation. Samples were taken at predetermined reaction times (30 s – 1 h) and analyzed for residual ozone by indigo,³⁴ *p*CBA by HPLC, and bromate by IC. R_{ct} , the ratio of concentrations of $\bullet OH$ and ozone, was determined as described previously³⁵ and used as a control parameter for comparing the different reaction conditions.

2.6. Quantum Chemical Computation. Aqueous-phase free energy (G_{aq}) of all species were obtained by the sum of electronic energy of a species solvated by explicit water molecules ($E_{0, gas}$), solvation free energy ($\Delta G_{solv, calc}$), and gaseous-phase correction for the explicit water molecules ($G_{corr, gas}$) (Text S12). $E_{0, gas}$ was calculated at the level of M06-2X/Aug-cc-pVTZ,³⁶ while $\Delta G_{solv, calc}$ and $G_{corr, gas}$ were calculated at the level of M06-2X/Aug-cc-pVDZ with an implicit

Table 1. Measured Apparent Second-Order Rate Constants at Indicated pH for the Reactions of the Selected Organic Model Compounds, Monochloramine, and a DOM Isolate with Br[•] (k_{Br^\bullet} , M⁻¹ s⁻¹ or (mgC/L)⁻¹ s⁻¹ for DOM) and Theoretically Calculated Free Energies of Activation ($\Delta G_{\text{aq,SET}}^{\text{act}}$, kcal mol⁻¹) for the Reactions of Organic Model Compounds and Monochloramine with Br[•] by Electron Transfer^a

compounds	group	pK _a	pH	measured k_{Br^\bullet} (this study) (average ± s.d.)	reported k_{Br^\bullet} (previous studies)	σ_p^{+e}	$\Delta G_{\text{aq,SET}}^{\text{act}}$ (kcal mol ⁻¹)
benzylamine	1° amine	9.3	10.0	$(7.4 \pm 0.5) \times 10^9$	n.a.		8.1
benzylamine	1° amine	9.3	7.1	$(3.8 \pm 0.01) \times 10^8$	n.a.		20.5
<i>N,N</i> -dimethylbenzylamine	3° amine	8.9	10.0	$(1.7 \pm 0.2) \times 10^{10}$	n.a.		3.1
<i>N,N</i> -dimethylbenzylamine	3° amine	8.9	7.1	$(9.1 \pm 5.5) \times 10^8$	n.a.		20.3
4-bromophenol	aromatic	9.1	10.0	$(2.8 \pm 0.7) \times 10^{10}$	n.a.	-2.15	0.1
4-bromophenol	aromatic	9.1	7.1	$(3.5 \pm 0.5) \times 10^9$	n.a.	-0.77	8.6
4-chlorophenol	aromatic	9.0	10.0	$(2.0 \pm 1.1) \times 10^{10}$	n.a.	-2.19	0.1
4-chlorophenol	aromatic	9.0	7.1	$(3.9 \pm 1.3) \times 10^9$	n.a.	-0.81	7.9
anisole	aromatic	n.a.	7.1	$(2.2 \pm 0.4) \times 10^9$	3.3×10^9 ¹⁰	-0.62	6.7
benzene ^b	aromatic	n.a.	7.1	3.4×10^8	n.a.	0	16.5
benzoic acid	aromatic	4.2	7.1	$(2.5 \pm 0.4) \times 10^8$	7.7×10^8 ¹⁰	-0.02	13.7
<i>p</i> -chlorobenzoic acid	aromatic	4.0	7.1	$(3.0 \pm 0.4) \times 10^8$	n.a.	0.09	14.9
ibuprofen ^c	aromatic	4.4	7.1	$(3.8 \pm 1.8) \times 10^9$	2.2×10^9 ¹²	-0.25	6.2
naphthalene	aromatic	n.a.	7.1	$(5.5 \pm 0.05) \times 10^9$	n.a.		5.7
phenol	aromatic	10.0	7.1	$(3.9 \pm 0.6) \times 10^9$	8.5×10^9 ¹⁰	-0.92	7.5
toluene ^d	aromatic	n.a.	7.1	4.5×10^8	n.a.	-0.31	11.1
3-phenylpropionic acid	aromatic	4.7	7.1	$(7.3 \pm 0.07) \times 10^8$	n.a.		11.8
<i>p</i> -benzoquinone	aromatic	n.a.	7.1	$(4.0 \pm 0.5) \times 10^9$	n.a.		41.2
sorbic acid	olefin	4.8	7.1	$(5.2 \pm 0.1) \times 10^9$	n.a.		5.0
<i>trans</i> -cinnamic acid	olefin	4.5	7.1	$(2.1 \pm 0.5) \times 10^9$	n.a.		7.6
monochloramine	inorganic	1.4	7.1	$(4.4 \pm 1.3) \times 10^9$	n.a.		3.8
SRFA	DOM	n.a.	7.1	$(1.7 \pm 0.01) \times 10^4$	2.6×10^4		n.a.
oxidized SRFA (0.8 gO3/gC)	DOM	n.a.	7.1	$(1.6 \pm 0.01) \times 10^4$	n.a.		n.a.
oxidized SRFA (1.5 gO3/gC)	DOM	n.a.	7.1	$(2.1 \pm 0.3) \times 10^4$	n.a.		n.a.

^aMost k_{Br^\bullet} were determined in competition with ibuprofen or unless otherwise indicated. k_{Br^\bullet} are shown as an average and standard deviation (s.d.) of duplicates except benzene and toluene. The corresponding competition kinetics plots are shown in Figure S5. ^bSingle measurement with a poor linearity of the competition kinetics plot ($R^2 = 0.67$, Figure S5). ^c k_{Br^\bullet} of ibuprofen was determined in competition with 4-iodophenol with k_{Br^\bullet} of 4-iodophenol of $6.6 \times 10^9 \text{ M}^{-1} \text{ s}^{-1}$. ^dSingle measurement. ^eAll σ_p^+ values were taken from Hansch et al.⁴⁰ except for ibuprofen, for which σ_p^+ was estimated after a structural approximation by Lee and von Gunten.⁴¹

solvation model (SMD)³⁷ and a continuum solvation method.³⁸ Methods were validated by experimentally determined reduction potentials for halides and aromatic compounds (Text S13). The aqueous free energy of reaction ($\Delta G_{\text{aq,SET}}^{\text{react}}$) was determined based on G_{aq} of reactants and products of the reaction, which was subsequently used for calculating free energy of activation ($\Delta G_{\text{aq}}^{\text{act}}$) by the Marcus theory³⁹ (Text S14).

3. RESULTS AND DISCUSSION

3.1. Reaction Kinetics. **3.1.1. Determination of k_{Br^\bullet} for Organic Model Compounds.** All k_{Br^\bullet} for organic model compounds, DOM, and NH₂Cl were determined by competition kinetics using ibuprofen as a competitor. k_{Br^\bullet} of ibuprofen was determined separately by competition kinetics with 4-iodophenol as a competitor. The reference k_{Br^\bullet} of 4-iodophenol was $(6.6 \pm 0.5) \times 10^9 \text{ M}^{-1} \text{ s}^{-1}$ based on the previous values determined by indirect methods using pulse radiolysis or laser flash photolysis.^{10,23} The obtained k_{Br^\bullet} of ibuprofen was $(4.6 \pm 1.4) \times 10^9 \text{ M}^{-1} \text{ s}^{-1}$ (duplicates), higher than the previously reported value of $2.2 \times 10^9 \text{ M}^{-1} \text{ s}^{-1}$ ¹² by a factor of 2. The final k_{Br^\bullet} of ibuprofen used as the reference was $(3.8 \pm 1.8) \times 10^9 \text{ M}^{-1} \text{ s}^{-1}$, an average of our measurements and the reported value. The relative standard deviation in the reference value is relatively large (48%), which systematically affects the results in this study. Table 1 shows that the selected organic model compounds have generally

high reactivity toward Br[•] with $k_{\text{Br}^\bullet} > 10^8 \text{ M}^{-1} \text{ s}^{-1}$. The determined k_{Br^\bullet} of anisole, benzoic acid, and phenol agree well to the reported values¹⁰ within a factor of <3, which is a typical error range for different kinetic studies. For some of the dissociating compounds, k_{Br^\bullet} was measured under two pH conditions (pH 7 and 10) to evaluate the effect of speciation on k_{Br^\bullet} . The species with higher electron density (e.g., phenolate and neutral amine) show a 5–20 times higher k_{Br^\bullet} than their protonated forms.

3.1.2. QSAR Models of k_{Br^\bullet} for Organic Model Compounds with σ_p^+ or $\Delta G_{\text{aq,SET}}^{\text{act}}$. To further validate the selectivity of Br[•], a QSAR was assessed for the measured k_{Br^\bullet} of the aromatic model compounds based on Hammett constant (specifically σ_p^+).^{40,41} Quantum-chemically (QC) computed free energies of activation, $\Delta G_{\text{aq,SET}}^{\text{act}}$, were also tested by assuming a single electron transfer as a reaction mechanism. The QSAR assessment results in a good correlation for both molecular descriptors ($R^2 = 0.82$ for σ_p^+ (Figure S7a) and $R^2 = 0.92$ for $\Delta G_{\text{aq,SET}}^{\text{act}}$ (Figure S7b)) for the aromatic group. Next, the QSAR approach was expanded to the other model compounds beyond aromatic groups and to the aromatic compounds for which Hammett constants are not available, by calculating $\Delta G_{\text{aq,SET}}^{\text{act}}$. The corresponding results are summarized in Table S8. An overall good QSAR for all model compounds including aromatic compounds (except *p*-benzoquinone), amines, olefins, and NH₂Cl was obtained ($R^2 = 0.77$, Figure 1). Four literature-reported k_{Br^\bullet} of phenol, ibuprofen, anisole, and

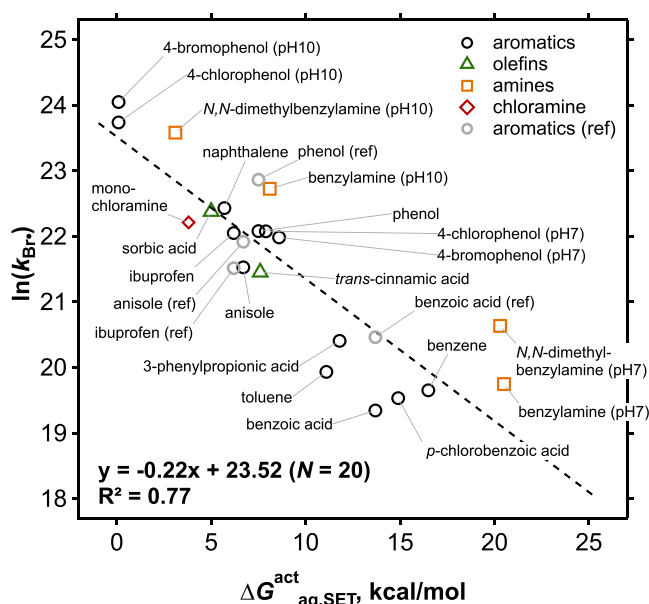


Figure 1. Quantitative structure–activity relationship of the measured second-order rate constants for the reactions of all selected model compounds (except *p*-benzoquinone) with Br^\bullet and the computed free energies of activation for electron transfer reactions (see Table 1). The aromatic compounds with reported k_{Br^\bullet} in the literature^{10,12} are labeled as “(ref)” and are also shown for comparison. The literature values were not included in the regression.

benzoic acid^{10,12} with our theoretically calculated $\Delta G_{\text{aq,SET}}^{\text{act}}$ values were included in Figure 1 to compare the correlation and they had only an insignificant impact on the overall trend. Because the QSAR was developed based on the $\Delta G_{\text{aq,SET}}^{\text{act}}$ assuming a single electron transfer, it supports a single electron transfer mechanism as the rate-determining step. Only *p*-benzoquinone appears to undergo a different reaction mechanism based on an exceedingly high $\Delta G_{\text{aq,SET}}^{\text{act}}$ value of 41.2 kcal/mol, significantly higher than for all the other compounds. Instead, *p*-benzoquinone seems to favor a Br^\bullet -addition mechanism to the aromatic ring, according to a lower $\Delta G_{\text{aq,addition}}^{\text{act}}$ of 4.8 kcal/mol.

3.1.3. k_{Br^\bullet} and Calculated $\Delta G_{\text{aq,SET}}^{\text{act}}$ for Ibuprofen. In addition to the simple organic model compounds, micropollutants also likely react by a single electron transfer mechanism, according to the result of ibuprofen agreeing well with the QSAR trend (Figure 1). The $\Delta G_{\text{aq,SET}}^{\text{act}}$ for ibuprofen was calculated as 6.2 kcal/mol, higher than the recently reported value (1.35 kcal/mol),¹² despite the use of the same DFT method (with a similar basis set) and the implicit solvation model. The discrepancy may have resulted from the accuracy of solvation energies for Br^- and Br^\bullet , which is critical to obtain an accurate $\Delta G_{\text{aq,SET}}^{\text{act}}$. Our calculation method was validated by calculating the one electron reduction potential of $\text{Br}^\bullet/\text{Br}^-$ with various DFT and *ab initio* methods and comparing the result with experimental values as a benchmark (Text S13). Such a validation process was not reported in the previous study.^{12,26} Another source of uncertainty is the treatment of the solvent reorganization energies in the Marcus theory calculations. Including both outer- and inner-sphere solvent reorganization energies is important because of the potential impacts of both reactants and surrounding water to the overall structure.

3.1.4. k_{Br^\bullet} and Calculated $\Delta G_{\text{aq,SET}}^{\text{act}}$ for NH_2Cl and Mechanistic Interpretation. NH_2Cl reacts fast with Br^\bullet with a k_{Br^\bullet} of $4.4 \times 10^9 \text{ M}^{-1} \text{ s}^{-1}$ (Table 1), higher than the reactivity of NH_2Cl with other radical species such as $\bullet\text{OH}$ ($k_{\bullet\text{OH},\text{NH}_2\text{Cl}} = 5.2 \times 10^8 \text{ M}^{-1} \text{ s}^{-1}$ or $5.7 \times 10^8 \text{ M}^{-1} \text{ s}^{-1}$).^{42,43} Previous studies on the reaction of NH_2Cl with $\bullet\text{OH}$ reported H-atom or Cl-atom abstraction as the main reaction mechanism. However, according to our computation results, for the reaction of NH_2Cl with Br^\bullet , a single electron transfer shows a clearly lower energy barrier than H-atom or Cl-atom abstraction ($\Delta G_{\text{aq}}^{\text{act}} = 3.8, 9.4, \text{ and } 19.2 \text{ kcal/mol}$, for electron transfer, H-atom abstraction, and Cl-atom abstraction, respectively). The good agreement of the experimental $k_{\text{Br}^\bullet,\text{NH}_2\text{Cl}}$ with the regression of the QSAR model built upon $\Delta G_{\text{aq,SET}}^{\text{act}}$ (Figure 1) also strongly supports a single electron transfer for the reaction of NH_2Cl with Br^\bullet . A single electron transfer reaction would form $\text{NH}_2\text{Cl}^{\bullet+}$ and Br^- as products, of which the former can dissociate to NHCl^\bullet . NHCl^\bullet is also formed in the reaction of NH_2Cl with $\bullet\text{OH}$ where self-decay or quenching reaction by dissolved oxygen were suggested as follow-up reactions.⁴²

3.1.5. Formation of Transient Adduct from Br^\bullet Reactions. Quantum-chemical computations additionally predicted the formation of an energetically stable transient adduct in the reaction coordinate to the oxidized target compound and Br^- (Figure S8). The formation of the adduct may not be a rate-determining step, but there is still a reasonable correlation between free energy of adduct formation ($\Delta G_{\text{aq}}^{\text{adduct}}$) and k_{Br^\bullet} (Figure S9). In most cases, the most energetically stable adduct among all possible conformers results from the interaction of a bromine atom (Br^\bullet) with a benzene ring (Table S7). Exceptions are the neutral forms of amine model compounds (benzylamine and *N,N*-dimethylbenzylamine) where Br^\bullet preferably interacts with the neutral amine-nitrogen over the benzene ring (nitrogen benzylamine- Br adduct $\Delta G_{\text{aq}}^{\text{adduct}} = -8.4 \text{ kcal/mol}$; adduct on the benzene ring: -1.1 kcal/mol). The preference on the amine-nitrogen was also illustrated by the spin density distribution of the protonated and deprotonated forms of amines (Table S9). For the protonated amines, the spin density is delocalized over the entire structure, indicating less favorable formation of an adduct ($\Delta G_{\text{aq}}^{\text{adduct}} = -0.4 \text{ kcal/mol}$ for the benzylamine- Br adduct). The $\Delta G_{\text{aq}}^{\text{adduct}}$ value of *p*-benzoquinone is higher than for other model compounds with similar k_{Br^\bullet} (e.g., $\Delta G_{\text{aq}}^{\text{adduct}} = 1.2 \text{ kcal/mol}$ for *p*-benzoquinone vs -1.9 kcal/mol for phenol (Table S7)), as observed also for $\Delta G_{\text{aq,SET}}^{\text{act}}$. The positive $\Delta G_{\text{aq}}^{\text{adduct}}$ value of *p*-benzoquinone indicates unfavorable interaction between Br^\bullet and the quinone structure due to the oxidized form of this compound.

3.1.6. Kinetics of Br^\bullet Reaction with DOM. The k_{Br^\bullet} for the DOM isolate SRFA II was determined as $(1.7 \pm 0.01) \times 10^4 \text{ (mgC/L)}^{-1} \text{ s}^{-1}$ (Table 1), matching to the previously reported value within a factor of < two ($k_{\text{Br}^\bullet} = 2.6 \times 10^4 \text{ (mgC/L)}^{-1} \text{ s}^{-1}$).²⁶ The determined value is close to the $k_{\bullet\text{OH}}$ of various types of DOM with an average value of $(2.2 \pm 0.8) \times 10^4 \text{ (mgC/L)}^{-1} \text{ s}^{-1}$,^{44–46} implying a similar DOM scavenging rate for Br^\bullet and $\bullet\text{OH}$. k_{Br^\bullet} of preozonated SRFA II was also determined to evaluate the effect of DOM oxidation during ozonation. Ozone targets electron-rich moieties of DOM (e.g., phenols),^{47–49} which are also reactive sites for Br^\bullet attack. The extent of preoxidation was controlled by measuring electron donating capacity (EDC), which characterizes antioxidant properties of DOM.⁴⁷ The oxidation of DOM with specific ozone doses of 0.8 gO_3/gC and 1.5 gO_3/gC led to a decrease

in EDC by $(31 \pm 5)\%$ and $(40 \pm 4)\%$, respectively (Text S2), agreeing with a previous observation.^{49,50} Nevertheless, $k_{\text{Br}\cdot}$ of non- and preozonated DOM remained in a similar range (Table 1), suggesting that DOM oxidation by ozone has a limited effect on its reactivity with $\text{Br}\cdot$ and its scavenging rate during ozonation. This is exemplified by *p*-benzoquinone, a major product of phenol oxidation by ozone,⁵¹ for which $k_{\text{Br}\cdot}$ is similar as for phenol (Table 1).

3.2. Product Formation and Reaction Mechanisms for the Reactions of Phenol with $\text{Br}\cdot$. **3.2.1. Identified Products.** Phenols are important DOM moieties and therefore phenol was selected to investigate product formation from the reaction with $\text{Br}\cdot$.⁴⁷ Its transformation products after reaction with $\text{Br}\cdot$ were investigated by LC-HRMS/MS and HPLC. Over a γ -irradiation time of 40 min (theoretically forming 22 μM $\text{Br}\cdot$, according to the dose rate), phenol was degraded by $\text{Br}\cdot$ from 21.7 μM to 17.6 μM , suggesting a 1:5 (phenol: $\text{Br}\cdot$) reaction stoichiometry (Figure S10). The reaction led to 2.4 μM *p*-benzoquinone, 0.5 μM hydroquinone, and 0.2 μM 4-bromophenol, as identified products. The sum of the residual concentrations of phenol and the concentrations of the identified products accounted for 96–98% of the initial phenol concentration. *p*-Benzoquinone was the major product with a yield of 59% per degraded phenol at 40 min, followed by hydroquinone (14%) and 4-bromophenol (4%) (Figure 2). A small concentration of catechol was also identified at the beginning of the reaction (0.1% at 12 min), but not for >12 min.

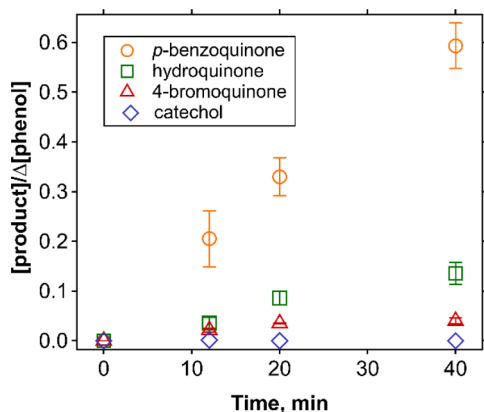


Figure 2. Relative product yields per degraded phenol as a function of the γ -radiolysis time during the reaction of phenol with $\text{Br}\cdot$, for the condition with 22 μM phenol, 0.7 mM 1,2-dibromoethane, 40 mM *t*-butanol, and 50 mM phosphate buffer (pH 7.1). Concentrations of phenol and the products as a function of time are provided in Figure S10.

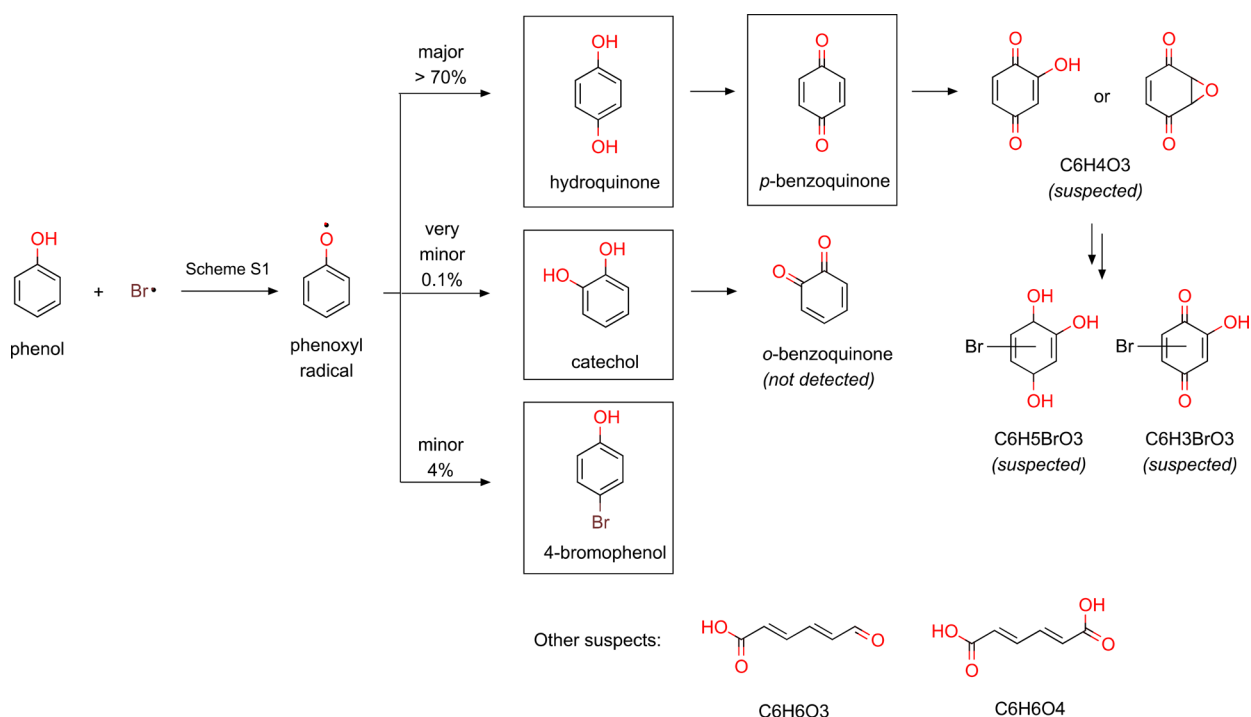
3.2.2. Suspected Products. In addition to the identified products with reference standards, some products were detected by nontargeted screenings of LC-HRMS/MS data where peaks with unique retention time and exact mass were extracted by comparing chromatograms of blank samples (containing phenol, no reaction) with those from γ -radiolysis samples (containing phenol, reaction with $\text{Br}\cdot$). Because the mass balance was almost complete by the identified products, they were minor products with yields <4%. Two suspected products featuring molecular formula of $\text{C}_6\text{H}_3\text{BrO}_3$ and $\text{C}_6\text{H}_5\text{BrO}_3$ were detected with a confidence level 3 (Text S15). They showed a gradual increase over time during γ -

radiolysis experiments with phenol and also *p*-benzoquinone (Figure S12), suggesting a presence of a quinone structure. For $\text{C}_6\text{H}_3\text{BrO}_3$, *p*-benzoquinone substituted by a hydroxy group and a Br was suggested as a possible molecular structure (Scheme 1) based on a comparison of MS spectra with a synthesized isomer (Text S15). The other suspected products consistently detected in the γ -radiolysis sample were: $\text{C}_6\text{H}_4\text{O}_3$, $\text{C}_{12}\text{H}_{10}\text{O}_2$, $\text{C}_6\text{H}_6\text{O}_3$, and $\text{C}_6\text{H}_6\text{O}_4$. $\text{C}_6\text{H}_4\text{O}_3$ is suspected as hydroxy-benzoquinone or benzoquinone-epoxide (Scheme 1) with a confidence level 3, which could be a precursor of $\text{C}_6\text{H}_3\text{BrO}_3$ and $\text{C}_6\text{H}_5\text{BrO}_3$. MS² spectra of $\text{C}_6\text{H}_4\text{O}_3$ featured a unique fragmentation pattern (Figure S14) but not specific enough to differentiate the two suspected structures (Figure S15). $\text{C}_{12}\text{H}_{10}\text{O}_2$ is likely to be dihydroxybiphenyl with a confidence level 2, based on the matching MS² pattern with a spectrum included in the MassBank spectral database (Figure S16).⁵² $\text{C}_6\text{H}_6\text{O}_3$ and $\text{C}_6\text{H}_6\text{O}_4$ are suspected as 6-oxo-2,4-hexylenedioic acid and muconic acid, respectively, but without sufficient evidence to confirm these structures (confidence level 4).

3.2.3. Phenol- $\text{Br}\cdot$ Reaction Mechanism. Based on the identified and suspected products, a reaction pathway of the reaction of phenol with $\text{Br}\cdot$ is proposed as in Scheme 1. Phenol is initially transformed by $\text{Br}\cdot$ to phenoxyl radical ($\text{PhO}\cdot$), analogously to its reaction with halogen dimer radical anions, $\text{X}_2^{\cdot-}$ ($\text{X} = \text{Cl}, \text{Br}, \text{I}$).⁵³ The presence of $\text{PhO}\cdot$ was supported by the detection of $\text{C}_{12}\text{H}_{10}\text{O}_2$ suspected to be dihydroxybiphenyl, often formed by dimerization of $\text{PhO}\cdot$.⁵³ The formation of $\text{PhO}\cdot$ can occur via electron transfer,^{10,54} H-abstraction,^{23,25} and Br-addition,²⁵ as depicted in Scheme S1. The QSARs of $k_{\text{Br}\cdot}$ determined by this study (Figure 1) supports an electron transfer reaction. After the initial step to $\text{PhO}\cdot$, the reaction pathway further branches to three reactions, resulting in hydroquinone, catechol, or 4-bromophenol, respectively, according to the identified products. Hydroquinone is the major product (>70%), based on the sum of the product yields of hydroquinone and *p*-benzoquinone (a subsequent oxidation product of hydroquinone). This is likely to further undergo hydroxylation and/or bromination reactions, leading to the suspected products ($\text{C}_6\text{H}_4\text{O}_3$, $\text{C}_6\text{H}_5\text{BrO}_3$, and $\text{C}_6\text{H}_3\text{BrO}_3$). The second pathway is a very minor pathway forming catechol (0.1% yield), a stereoisomer of hydroquinone which was only detected at a short reaction time (12 min). It may be further oxidized to *o*-benzoquinone, which is difficult to confirm because of its poor stability in aqueous solution.⁵⁵ The third pathway with 4% yield of 4-bromophenol may imply a possible addition mechanism comparable to the oxidation of phenol by $\cdot\text{OH}$ (Scheme S1(3))⁵⁶ or a radical–radical coupling mechanism of $\text{PhO}\cdot$ and $\text{Br}\cdot$ confirmed by calculated thermodynamically favorable $\Delta G_{\text{aq}}^{\text{react}}$ (Text S16). In addition to ring products, ring-opening products such as 6-oxo-2,4-hexylenedioic acid and muconic acid are also suspected (Scheme 1). Such short-chain organic acids (up to C_6) were identified during oxidation of phenol by $\cdot\text{OH}$ ^{57,58} and ozone.⁵⁹ Dicarbonyl compounds were also reported as ring-opening products from the reaction of phenol with chlorine and $\cdot\text{OH}$,^{60,61} but they could not be detected by the analytical method applied in this study.

3.3. Mitigation of Bromate Formation by Monochloramine during Ozonation: Role of $\text{Br}\cdot$. As a proven strategy to mitigate bromate during ozonation,¹⁸ the chlorine-ammonia pretreatment blocks the initial steps of bromate formation by masking bromide and scavenging $\cdot\text{OH}$ (Text S17). As an

Scheme 1. Reaction Pathway for the Reaction of Phenol with Br^\bullet Based on the Identified (in squares) and Suspected Products^a



^aThe initial step of forming phenoxyl radical is described in detail in Scheme S1.

alternative, a simpler strategy has been applied, which entails the direct addition of NH_2Cl before ozonation. It has an advantage over the chlorine-ammonia process by forming less chlorinated DBPs by avoiding free chlorine contact time. Quenching of $\bullet\text{OH}$ by NH_2Cl is similar to the chlorine-ammonia process. However, an additional benefit such as bromide masking is not expected, because the reaction of NH_2Cl with bromide is slow ($k = 0.14 \text{ M}^{-1} \text{ s}^{-1}$ at pH 7).³⁰ According to our measurement, NH_2Cl reacts fast with Br^\bullet with k_{Br^\bullet} of $4.4 \times 10^9 \text{ M}^{-1} \text{ s}^{-1}$ and may therefore be a quencher for this transient species. Additionally, NH_2Cl reacts with HOBr with $k = 2.8 \times 10^5 \text{ M}^{-1} \text{ s}^{-1}$ at pH 7.^{4,62} This may also add to bromate mitigation, however, only when HOBr significantly builds up during ozonation.

To assess the effect of NH_2Cl in quenching Br^\bullet , the fraction of Br^\bullet reacting with a compound X, $f(\text{Br}^\bullet + \text{X})$, was calculated based on the measured and reported values for k_{Br^\bullet} of NH_2Cl , DOM, ozone, and bromide, which are considered the main Br^\bullet consumers during ozonation (Text S18). Figure 3 shows the calculated $f(\text{Br}^\bullet + \text{X})$ in absence or presence of NH_2Cl for low dissolved organic carbon (DOC) and Br^- levels as in typical Swiss surface waters. Without NH_2Cl , most Br^\bullet was quenched by DOM (Figure 3a). The low DOC concentration (1 mgC/L) was yet high enough to quench at least 84% of Br^\bullet for a range of specific ozone doses of 0.5–1.0 mgO_3/mgC , typically applied in drinking water treatment in Switzerland (shaded area in Figure 3). For the same conditions, $f(\text{Br}^\bullet + \text{O}_3)$ and $f(\text{Br}^\bullet + \text{Br}^-)$ were 8–15% and 0.03%, respectively. The result was markedly changed in the presence of 15 μM NH_2Cl where NH_2Cl became the major consumer scavenging at least 70% of Br^\bullet even for the highest ozone dose of 60 μM . Under these conditions, $f(\text{Br}^\bullet + \text{DOM})$ was reduced to 20% and more importantly $f(\text{Br}^\bullet + \text{O}_3)$ was reduced to 2–4%. This demonstrates, that the $\text{Br}^\bullet + \text{O}_3$ reaction is significantly suppressed by

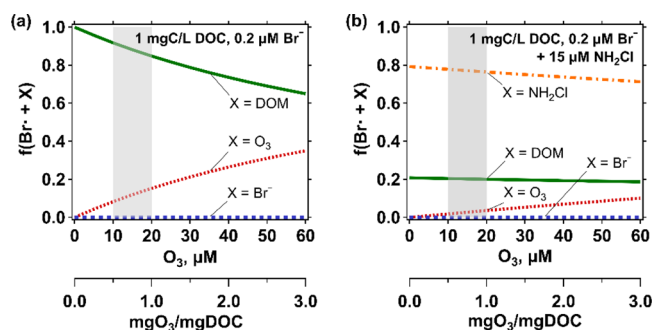


Figure 3. Calculated fractions (see text) of Br^\bullet reacting with DOM (green line), ozone (red line), bromide (blue line), or NH_2Cl (orange line) as a function of ozone concentration in the (a) absence or (b) presence of NH_2Cl . The selected concentrations were 1 mgC/L DOC, 0.2 μM Br^- (16 $\mu\text{g}/\text{L}$ Br^-), and 15 μM NH_2Cl . Shaded areas indicate a typical range of ozone doses applied in drinking water treatment in Switzerland (0.5–1.0 mgO_3/mgC).

a factor of 4. Conditions with higher DOC and Br^- levels simulating wastewater were also assessed and the results are shown in Figure S18. For these conditions, DOM plays an important role even in the presence of 15 μM NH_2Cl , quenching 53–57% of Br^\bullet for the entire range of ozone concentrations. Therefore, the quenching effect by NH_2Cl in the water with high DOC levels is not expected as significant as in the water with low DOC concentrations. Nevertheless, the $f(\text{Br}^\bullet + \text{O}_3)$ decreases by a factor of 2, which still mitigates the reaction between Br^\bullet and ozone significantly. Br^- does not influence the Br^\bullet concentration based on the low $f(\text{Br}^\bullet + \text{Br}^-)$ of 0.1–0.2%, even with the higher Br^- level of 1.3 μM (or 100 $\mu\text{g}/\text{L}$). The importance of DOM relative to the other consumers (ozone and Br^-) is additionally illustrated by

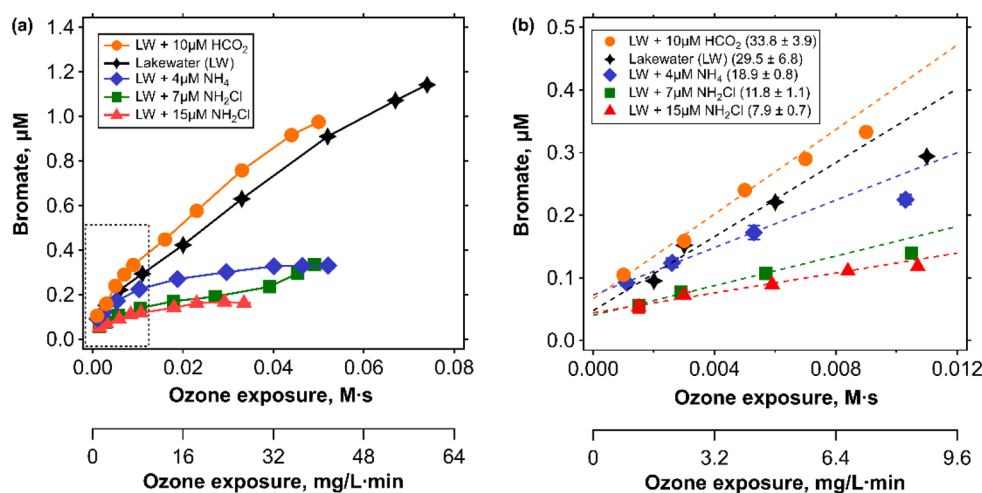


Figure 4. (a) Bromate formation as a function of the ozone exposure for five ozonation conditions. Unaltered Lake Zurich water contained 1.4 mgC/L DOC, 2 μM bromide, 1 mM phosphate buffer (pH 7.6), 5 μM pCBA, and a 60 μM ozone dose (black four pointed stars). The other conditions additionally contained 10 μM formate (orange circles), 4 μM ammonium (blue diamonds), 7 μM NH_2Cl (green squares), or 15 μM NH_2Cl (red triangles), respectively. (b) A close-up for a low range of ozone exposures (dotted rectangle in a). The slopes of the first three data points are provided in Table 2.

Table 2. Conditions of Ozonation Experiments with Lake Zurich Water (1.4 mgC/L DOC, 2.7 mM Alkalinity, 2 μM Bromide (spiked), 0.5 μM pCBA (spiked), 1 mM Phosphate Buffer at pH 7.6 (spiked)) and the Determined R_{ct} (Figure 20a), the Bromate Formation Slopes Expressed As a Function of Ozone Exposure, And the Change in Bromate Formation with Regard to the Reference Conditions

no.	condition	comment	R_{ct}	slope ($\mu\text{M}/(\text{M s})^{\text{a}}$)	change in bromate formation ^b (%)	reference condition
1	Lake Zurich water (unaltered)	reference for low R_{ct}	3.7×10^{-9}	29.5 ± 6.8		
2	Lake Zurich water + 10 μM formate	reference for high R_{ct}	7.4×10^{-9}	33.8 ± 3.9	+15	1
3	Lake Zurich water + 4 μM NH_4^+	NH_4^+ as HOBr quencher	4.3×10^{-9}	18.9 ± 0.8	-36	1
4	Lake Zurich water + 7 μM NH_2Cl	NH_2Cl as HOBr/ Br^\bullet quencher	5.6×10^{-9}	11.8 ± 1.1	-60	1
5	Lake Zurich water + 15 μM NH_2Cl	NH_2Cl as HOBr/ Br^\bullet quencher	9.9×10^{-9}	7.9 ± 0.7	-73	1
					-77	2
					-58	3

^aSlopes were obtained from linear regression of a bromate concentration plot as a function of ozone exposure for the initial phase (Figure 4b).

^bChanges in bromate formation were obtained by comparing the slope of a condition with the slope of a reference condition specified in the last column.

plotting $f(\text{Br}^\bullet + \text{NH}_2\text{Cl})$ as a function of bromide, ozone, or DOC concentration. Figure S19 shows that $f(\text{Br}^\bullet + \text{NH}_2\text{Cl})$ remains almost constant throughout the range of bromide and ozone concentrations, whereas it changes as a function of the DOC concentration.

The Br^\bullet quenching effect by NH_2Cl was further assessed experimentally by measuring bromate formation during ozonation in presence or absence of NH_2Cl in a lake water. Figure 4 shows the bromate formation during ozonation of Lake Zurich water containing 1.4 mgC/L DOC, spiked with 2 μM of bromide, with a 60 μM ozone dose at pH 7.6 as a function of the ozone exposure (black four pointed stars). Additional experiments are shown for addition of NH_2Cl (green squares (7 μM), red triangles (15 μM)), formate (orange circles), or ammonium (blue diamonds) to Lake Zurich water. Fifteen μM NH_2Cl theoretically quenches 66% of Br^\bullet , based on the calculated $f(\text{Br}^\bullet + \text{NH}_2\text{Cl})$, shown by the red asterisk in Figure S19. Oxidant exposures (ozone and $\bullet\text{OH}$) of the different conditions were assessed by measuring R_{ct} , the ratio of $\bullet\text{OH}$ exposure to ozone exposure.³⁵ The corresponding R_{ct} values for each condition are provided in Table 2 and Figure S20a and the ozone decay curves are shown

in Figure S20b. To compare bromate formation among the different conditions, slopes of the bromate formation curves were obtained by linear regression of the initial formation (Figure 4b). The reduction in bromate formation of a quenching condition was calculated by comparing the slope of a quenching condition with the slope of a reference condition (Table 2). The addition of 7 μM NH_2Cl reduced bromate by 60% compared to the unaltered Lake Zurich water. Doubling the NH_2Cl concentration to 15 μM enhanced the reduction of bromate formation to 73%. However, for 15 μM NH_2Cl , the R_{ct} increased from 5.6×10^{-9} to 9.9×10^{-9} (Table 2), due to additional consumption of ozone and $\bullet\text{OH}$ by NH_2Cl ($k_{\text{O}_3} = 26 \text{ M}^{-1} \text{ s}^{-1}$ and $k_{\bullet\text{OH}} = 5.2 \times 10^8 \text{ M}^{-1} \text{ s}^{-1}$ or $5.7 \times 10^8 \text{ M}^{-1} \text{ s}^{-1}$).^{19,42,43} To mimic this change in R_{ct} , another reference condition was tested by using 10 μM formate, which promotes ozone decay by forming $\text{O}_2^{\bullet-}$ and thereby increases R_{ct} .⁶³ The R_{ct} of the new reference condition with formate was 7.4×10^{-9} , very close to the 15 μM NH_2Cl condition. Based on this comparison, the bromate mitigation for 15 μM NH_2Cl was updated to 77% relative to the formate addition. The bromate formation of the reference condition with formate was augmented by 15% relative to the unaltered Lake Zurich water. This can be explained by the higher R_{ct} in the presence of

formate (similar to 15 μM NH_2Cl), indicating higher $\bullet\text{OH}$ exposure at a given ozone exposure, resulting in higher overall oxidant exposure and bromate. In contrast, an increase in R_{ct} from 7 μM to 15 μM NH_2Cl suppressed the bromate formation, in agreement with the $\text{Br}\bullet$ quenching effect by NH_2Cl .

In addition to the NH_2Cl experiment, ammonium (NH_4^+) was tested to further confirm the effect of quenching $\text{Br}\bullet/\text{HOBr}$ on bromate formation. NH_2Cl quenches HOBr as well as $\text{Br}\bullet$ ($k_{\text{Br}\bullet} = 4.4 \times 10^9 \text{ M}^{-1} \text{ s}^{-1}$ (Table 1) and $k_{\text{HOBr}} = 2.8 \times 10^5 \text{ M}^{-1} \text{ s}^{-1}$ at pH 7),^{4,62} $\text{NH}_4^+/\text{NH}_3$ only quenches HOBr ($k_{\text{Br}\bullet} \ll 9.7 \times 10^7 \text{ M}^{-1} \text{ s}^{-1}$, assumed based on $k_{\bullet\text{OH}}$ of NH_3 (generally more reactive species than NH_4^+)⁶⁴ and $k_{\text{HOBr}} \sim 10^6 \text{ M}^{-1} \text{ s}^{-1}$ at pH 7–8).⁴ An NH_4^+ concentration of 4 μM was selected to obtain a similar HOBr quenching rate as for 15 μM NH_2Cl . The condition with 4 μM NH_4^+ (blue diamonds) leads to a reduction of bromate formation by 36%, mainly due to quenching of HOBr . Therefore, from the 73% bromate mitigation observed for 15 μM NH_2Cl , roughly similar contributions can be attributed to the quenching of HOBr and $\text{Br}\bullet$, respectively. The reduction of bromate formation by 15 μM NH_2Cl compared to by NH_4^+ was 58% (by taking the NH_4^+ condition as reference) and occurred mainly during the initial phase of the ozonation (Figure 4b). During this phase, an enhanced $\text{Br}\bullet$ formation is expected from the reaction of bromide with $\bullet\text{OH}$, which are formed in high concentrations during the initial phase of an ozonation.^{29,65} Therefore, quenching of $\text{Br}\bullet$ by NH_2Cl during the initial phase slows down bromate formation by reducing the transient $\text{Br}\bullet$ concentrations.

3.4. Practical Implications. The good correlation of the experimentally determined $k_{\text{Br}\bullet}$ with the molecular descriptors (Hammett constants and the computed $\Delta G^{\text{act}}_{\text{aq,SET}}$) for diverse functional groups (aromatics, amines, olefins, and NH_2Cl) enables a prediction of $k_{\text{Br}\bullet}$ for a wider range of compounds. As shown by the case of *p*-benzoquinone, some compounds react with $\text{Br}\bullet$ by different mechanisms than common aromatic rings (e.g., addition instead of electron transfer), which needs further investigation to improve prediction capability for such compounds. The predominant formation of hydroquinone (and subsequently *p*-benzoquinone) during the phenol- $\text{Br}\bullet$ reaction raises concern related to mutagenicity. Their formation is comparable to the phenol reaction with other oxidants (e.g., ozone, $\bullet\text{OH}$) and likely to follow similar subsequent reactions to ring opening compounds. In addition to quinones, brominated phenol was identified during the phenol- $\text{Br}\bullet$ reaction but as a minor product only. Accordingly, only a small fraction of $\text{Br}\bullet$ will react with DOM to form Br-DBPs, which is likely to be outweighed by other sources of Br-DBP such as bromination of DOM by HOBr . During conventional ozonation, $\text{Br}\bullet$ plays a key role in bromate formation by its further reaction with ozone. According to our kinetic result, this reaction can be partially inhibited by the fast reaction of $\text{Br}\bullet$ with DOM. For a typical Swiss surface waters with the DOC concentration of $\sim 1 \text{ mgC/L}$, the majority of $\text{Br}\bullet$ is quenched by DOM and the rest reacts with ozone. Despite the generally small fraction, the oxidation of $\text{Br}\bullet$ by ozone can lead to a substantial portion of formed bromate, especially during an initial phase of ozonation where $\bullet\text{OH}$ exposure is high and $\text{Br}\bullet$ becomes an important bromate precursor. This bromate formation pathway involving $\text{Br}\bullet$ can be suppressed by NH_2Cl , according to our theoretical and experimental assessment. It was demonstrated that the majority of $\text{Br}\bullet$ can

be quenched by 15 μM NH_2Cl for the condition with DOC concentrations on the order of 1–2 mgC/L. Accordingly, bromate reduction of 70–80% was achieved during ozonation of real Lake water even with the excess ozone dose applied in this study (corresponding to $\sim 2 \text{ gO}_3/\text{gC}$). About a half of the reduction was related to quenching of $\text{Br}\bullet$ and the other was linked to quenching of HOBr . Overall, NH_2Cl can interfere in both the $\bullet\text{OH}$ (forming $\text{Br}\bullet$) and ozone pathway (forming HOBr), serving as an efficient quenching agent throughout the course of ozonation. Additional benefits of the NH_2Cl treatment over the chlorine-ammonia treatment prior to ozonation is mitigating the formation of chlorinated and brominated DBPs, because of a lower reactivity of NH_2Cl with DOM and with Br^- . The NH_2Cl pretreatment would be less efficient for waters with higher DOC concentrations ($\sim 5 \text{ mg/L}$) such as wastewater, but the fraction of $\text{Br}\bullet$ oxidized by ozone can be suppressed by a factor of 2, which results in a significant reduction in bromate. If the advanced oxidation processes UV/ H_2O_2 is applied in Br^- -containing water, Br^- can scavenge $\bullet\text{OH}$ to form $\text{Br}\bullet$. However, even for wastewater featuring elevated Br^- levels, DOM still quenches about 99% of the $\bullet\text{OH}$ (based on 1 μM Br^- , 4 mgC/L DOC and $k_{\bullet\text{OH}} = (2.2 \pm 0.8) \times 10^4 (\text{mgC/L})^{-1} \text{ s}^{-1}$ for DOM^{44-46} and $1.1 \times 10^9 \text{ M}^{-1} \text{ s}^{-1}$ for Br^- to $\text{Br}\bullet$).²¹ Because only a minor fraction of $\text{Br}\bullet$ leads to Br-DBPs, small changes are expected in the process performance.

■ ASSOCIATED CONTENT

Supporting Information

The Supporting Information is available free of charge at <https://pubs.acs.org/doi/10.1021/acs.est.2c07694>.

Supplementary texts, figures, tables, and scheme to further describe the materials and methods and corroborate results and discussion (PDF)

■ AUTHOR INFORMATION

Corresponding Author

Urs von Gunten – Eawag, Swiss Federal Institute of Aquatic Science and Technology, Dübendorf 8600, Switzerland; School of Architecture, Civil and Environmental Engineering (ENAC), École Polytechnique Fédérale de Lausanne (EPFL), Lausanne 1015, Switzerland; Email: vongunten@eawag.ch

Authors

Sungeun Lim – Eawag, Swiss Federal Institute of Aquatic Science and Technology, Dübendorf 8600, Switzerland; Present Address: Department of Civil and Environmental Engineering, Stanford University, 473 Via Ortega, Stanford, CA 94305, United States

Benjamin Barrios – Department of Civil and Environmental Engineering, Michigan Technological University, Houghton, Michigan 49931, United States

Daisuke Minakata – Department of Civil and Environmental Engineering, Michigan Technological University, Houghton, Michigan 49931, United States; orcid.org/0000-0003-3055-3880

Complete contact information is available at: <https://pubs.acs.org/doi/10.1021/acs.est.2c07694>

Notes

The authors declare no competing financial interest.

ACKNOWLEDGMENTS

This research was funded by the Swiss National Science Foundation (project no. 200021-181975). We thank Paul Scherrer Institute (PSI) for access to the γ -radiolysis facility, Viktor Boutellier at PSI for technical support, Jakob Helbing at Zurich Water Supply for help in collecting Lake Zurich water, the AuA Laboratory at Eawag for analyses of general water quality parameters, Samuel Derrer at Eawag for chemical synthesis, and Elisabeth Muck at Eawag for laboratory support. B.B. and D.M. were partially supported by NSF CHM-1808052. D.M. acknowledges the support by Eawag during his sabbatical.

REFERENCES

- (1) Soltermann, F.; Abegglen, C.; Götz, C.; von Gunten, U. Bromide Sources and Loads in Swiss Surface Waters and Their Relevance for Bromate Formation during Wastewater Ozonation. *Environ. Sci. Technol.* **2016**, *50* (18), 9825–9834.
- (2) Flury, M.; Papritz, A. Bromide in the Natural Environment: Occurrence and Toxicity. *Journal of Environmental Quality* **1993**, *22* (4), 747–758.
- (3) von Gunten, U. Oxidation Processes in Water Treatment: Are We on Track? *Environ. Sci. Technol.* **2018**, *52* (9), 5062–5075.
- (4) Heeb, M. B.; Criquet, J.; Zimmermann-Steffens, S. G.; von Gunten, U. Oxidative Treatment of Bromide-Containing Waters: Formation of Bromine and Its Reactions with Inorganic and Organic Compounds — A Critical Review. *Water Res.* **2014**, *48*, 15–42.
- (5) Grebel, J. E.; Pignatello, J. J.; Mitch, W. A. Effect of Halide Ions and Carbonates on Organic Contaminant Degradation by Hydroxyl Radical-Based Advanced Oxidation Processes in Saline Waters. *Environ. Sci. Technol.* **2010**, *44* (17), 6822–6828.
- (6) Lee, W.; Lee, Y.; Allard, S.; Ra, J.; Han, S.; Lee, Y. Mechanistic and Kinetic Understanding of the UV254 Photolysis of Chlorine and Bromine Species in Water and Formation of Oxyhalides. *Environ. Sci. Technol.* **2020**, *54* (18), 11546–11555.
- (7) von Gunten, U.; Oliveras, Y. Advanced Oxidation of Bromide-Containing Waters: Bromate Formation Mechanisms. *Environ. Sci. Technol.* **1998**, *32* (1), 63–70.
- (8) Richardson, S. D.; Thruston, A. D.; Rav-Acha, C.; Groisman, L.; Popilevsky, I.; Juraev, O.; Glezer, V.; McKague, A. B.; Plewa, M. J.; Wagner, E. D. Tribromopyrrole, Brominated Acids, and Other Disinfection Byproducts Produced by Disinfection of Drinking Water Rich in Bromide. *Environ. Sci. Technol.* **2003**, *37* (17), 3782–3793.
- (9) Langsa, M.; Heitz, A.; Joll, C. A.; von Gunten, U.; Allard, S. Mechanistic Aspects of the Formation of Adsorbable Organic Bromine during Chlorination of Bromide-Containing Synthetic Waters. *Environ. Sci. Technol.* **2017**, *51* (9), 5146–5155.
- (10) Lei, Y.; Lei, X.; Yu, Y.; Li, K.; Li, Z.; Cheng, S.; Ouyang, G.; Yang, X. Rate Constants and Mechanisms for Reactions of Bromine Radicals with Trace Organic Contaminants. *Environ. Sci. Technol.* **2021**, *55* (15), 10502–10513.
- (11) Cheng, S.; Zhang, X.; Yang, X.; Shang, C.; Song, W.; Fang, J.; Pan, Y. The Multiple Role of Bromide Ion in PPCPs Degradation under UV/Chlorine Treatment. *Environ. Sci. Technol.* **2018**, *52* (4), 1806–1816.
- (12) Guo, K.; Zheng, S.; Zhang, X.; Zhao, L.; Ji, S.; Chen, C.; Wu, Z.; Wang, D.; Fang, J. Roles of Bromine Radicals and Hydroxyl Radicals in the Degradation of Micropollutants by the UV/Bromine Process. *Environ. Sci. Technol.* **2020**, *54* (10), 6415–6426.
- (13) Parker, K. M.; Mitch, W. A. Halogen Radicals Contribute to Photooxidation in Coastal and Estuarine Waters. *Proc. Natl. Acad. Sci. U.S.A.* **2016**, *113* (21), 5868–5873.
- (14) Parker, K. M.; Reichwaldt, E. S.; Ghadouani, A.; Mitch, W. A. Halogen Radicals Promote the Photodegradation of Microcystins in Estuarine Systems. *Environ. Sci. Technol.* **2016**, *50* (16), 8505–8513.
- (15) von Gunten, U.; Hoigne, J. Bromate Formation during Ozonation of Bromide-Containing Waters: Interaction of Ozone and Hydroxyl Radical Reactions. *Environ. Sci. Technol.* **1994**, *28* (7), 1234–1242.
- (16) *National Primary Drinking Water Regulations*. U.S. EPA. <https://www.epa.gov/ground-water-and-drinking-water/national-primary-drinking-water-regulations> (accessed 2022-09-05).
- (17) EU. Directive (EU) 2020/2184 of the European Parliament and of the Council of 16 December 2020 on the Quality of Water Intended for Human Consumption (Recast). *Official Journal of the European Union* **2020**, L435, 1–62.
- (18) von Sonntag, C.; von Gunten, U. *Chemistry of Ozone in Water and Wastewater Treatment*; IWA Publishing, 2012.
- (19) Haag, W. R.; Hoigné, J. Ozonation of Bromide-Containing Waters: Kinetics of Formation of Hypobromous Acid and Bromate. *Environ. Sci. Technol.* **1983**, *17* (5), 261–267.
- (20) Liu, Q.; Schurter, L. M.; Muller, C. E.; Aloisio, S.; Francisco, J. S.; Margerum, D. W. Kinetics and Mechanisms of Aqueous Ozone Reactions with Bromide, Sulfite, Hydrogen Sulfite, Iodide, and Nitrite Ions. *Inorg. Chem.* **2001**, *40* (17), 4436–4442.
- (21) Zehavi, D.; Rabani, J. Oxidation of Aqueous Bromide Ions by Hydroxyl Radicals. Pulse Radiolytic Investigation. *J. Phys. Chem.* **1972**, *76* (3), 312–319.
- (22) Kläning, U. K.; Wolff, T. Laser Flash Photolysis of HClO, ClO⁻, HBrO, and BrO⁻ in Aqueous Solution. Reactions of Cl⁻ and Br⁻ Atoms. *Berichte der Bunsengesellschaft für physikalische Chemie* **1985**, *89* (3), 243–245.
- (23) Merényi, G.; Lind, J. Reaction Mechanism of Hydrogen Abstraction by the Bromine Atom in Water. *J. Am. Chem. Soc.* **1994**, *116* (17), 7872–7876.
- (24) Scaiano, J. C.; Barra, M.; Krzywinski, M.; Sinta, R.; Calabrese, G. Laser Flash Photolysis Determination of Absolute Rate Constants for Reactions of Bromine Atoms in Solution. *J. Am. Chem. Soc.* **1993**, *115* (18), 8340–8344.
- (25) Guha, S. N.; Schoneich, C.; Asmus, K. D. Free Radical Reductive Degradation of Vic-Dibromoalkanes and Reaction of Bromine Atoms with Polyunsaturated Fatty Acids: Possible Involvement of Br[•] in the 1,2-Dibromoethane-Induced Lipid Peroxidation. *Arch. Biochem. Biophys.* **1993**, *305* (1), 132–140.
- (26) Lei, Y.; Lei, X.; Westerhoff, P.; Tong, X.; Ren, J.; Zhou, Y.; Cheng, S.; Ouyang, G.; Yang, X. Bromine Radical (Br[•] and Br₂^{•-}) Reactivity with Dissolved Organic Matter and Brominated Organic Byproduct Formation. *Environ. Sci. Technol.* **2022**, *56* (8), 5189–5199.
- (27) Pearce, R.; Hogard, S.; Buehlmann, P.; Salazar-Benites, G.; Wilson, C.; Bott, C. Evaluation of Preformed Monochloramine for Bromate Control in Ozonation for Potable Reuse. *Water Res.* **2022**, *211*, 118049.
- (28) Ling, L.; Deng, Z.; Fang, J.; Shang, C. Bromate Control during Ozonation by Ammonia-Chlorine and Chlorine-Ammonia Pretreatment: Roles of Bromine-Containing Haloamines. *Chemical Engineering Journal* **2020**, *389*, 123447.
- (29) Pinkernell, U.; von Gunten, U. Bromate Minimization during Ozonation: Mechanistic Considerations. *Environ. Sci. Technol.* **2001**, *35* (12), 2525–2531.
- (30) Luh, J.; Mariñas, B. J. Kinetics of Bromochloramine Formation and Decomposition. *Environ. Sci. Technol.* **2014**, *48* (5), 2843–2852.
- (31) Lal, M.; Mahal, H. S. Reactions of Alkylbromides with Free Radicals in Aqueous Solutions. *International Journal of Radiation Applications and Instrumentation. Part C. Radiation Physics and Chemistry* **1992**, *40* (1), 23–26.
- (32) Lal, M.; Mönig, J.; Asmus, K.-D.; Wardman, P. Free Radical Induced Degradation of 1, 2-Dibromoethane. Generation of Free Br[•] and Br₂^{•-} Atoms. *Free Radical Res. Commun.* **1986**, *1* (4), 235–241.
- (33) Schymanski, E. L.; Jeon, J.; Gulde, R.; Fenner, K.; Ruff, M.; Singer, H. P.; Hollender, J. Identifying Small Molecules via High Resolution Mass Spectrometry: Communicating Confidence. *Environ. Sci. Technol.* **2014**, *48* (4), 2097–2098.

- (34) Bader, H.; Hoigné, J. Determination of Ozone in Water by the Indigo Method. *Water Res.* **1981**, *15* (4), 449–456.
- (35) Elovitz, M. S.; von Gunten, U. Hydroxyl Radical/Ozone Ratios During Ozonation Processes. I. The Rct Concept. *Ozone: Science & Engineering* **1999**, *21* (3), 239–260.
- (36) Zhao, Y.; Truhlar, D. G. The M06 Suite of Density Functionals for Main Group Thermochemistry, Thermochemical Kinetics, Noncovalent Interactions, Excited States, and Transition Elements: Two New Functionals and Systematic Testing of Four M06-Class Functionals and 12 Other Functionals. *Theor. Chem. Acc.* **2008**, *120* (1), 215–241.
- (37) Marenich, A. V.; Cramer, C. J.; Truhlar, D. G. Universal Solvation Model Based on Solute Electron Density and on a Continuum Model of the Solvent Defined by the Bulk Dielectric Constant and Atomic Surface Tensions. *J. Phys. Chem. B* **2009**, *113* (18), 6378–6396.
- (38) Bryantsev, V. S.; Diallo, M. S.; Goddard, W. A., III Calculation of Solvation Free Energies of Charged Solutes Using Mixed Cluster/Continuum Models. *J. Phys. Chem. B* **2008**, *112* (32), 9709–9719.
- (39) Marcus, R. A. Chemical and Electrochemical Electron-Transfer Theory. *Annu. Rev. Phys. Chem.* **1964**, *15* (1), 155–196.
- (40) Hansch, C.; Leo, A.; Taft, R. W. A Survey of Hammett Substituent Constants and Resonance and Field Parameters. *Chem. Rev.* **1991**, *91* (2), 165–195.
- (41) Lee, Y.; von Gunten, U. Quantitative Structure-Activity Relationships (QSARs) for the Transformation of Organic Micropollutants during Oxidative Water Treatment. *Water Res.* **2012**, *46* (19), 6177–6195.
- (42) Poskrebyshev, G. A.; Huie, R. E.; Neta, P. Radiolytic Reactions of Monochloramine in Aqueous Solutions. *J. Phys. Chem. A* **2003**, *107* (38), 7423–7428.
- (43) Gleason, J. M.; McKay, G.; Ishida, K. P.; Mezyk, S. P. Temperature Dependence of Hydroxyl Radical Reactions with Chloramine Species in Aqueous Solution. *Chemosphere* **2017**, *187*, 123–129.
- (44) Brezonik, P. L.; Fulkerson-Brekken, J. Nitrate-Induced Photolysis in Natural Waters: Controls on Concentrations of Hydroxyl Radical Photo-Intermediates by Natural Scavenging Agents. *Environ. Sci. Technol.* **1998**, *32* (19), 3004–3010.
- (45) Katsoyiannis, I. A.; Canonica, S.; von Gunten, U. Efficiency and Energy Requirements for the Transformation of Organic Micropollutants by Ozone, O₃/H₂O₂ and UV/H₂O₂. *Water Res.* **2011**, *45* (13), 3811–3822.
- (46) Westerhoff, P.; Mezyk, S. P.; Cooper, W. J.; Minakata, D. Electron Pulse Radiolysis Determination of Hydroxyl Radical Rate Constants with Suwannee River Fulvic Acid and Other Dissolved Organic Matter Isolates. *Environ. Sci. Technol.* **2007**, *41* (13), 4640–4646.
- (47) Houska, J.; Salhi, E.; Walpen, N.; von Gunten, U. Oxidant-Reactive Carbonous Moieties in Dissolved Organic Matter: Selective Quantification by Oxidative Titration Using Chlorine Dioxide and Ozone. *Water Res.* **2021**, *207*, 117790.
- (48) Lim, S.; Shi, J. L.; von Gunten, U.; McCurry, D. L. Ozonation of Organic Compounds in Water and Wastewater: A Critical Review. *Water Res.* **2022**, *213*, 118053.
- (49) Önnby, L.; Salhi, E.; McKay, G.; Rosario-Ortiz, F. L.; von Gunten, U. Ozone and Chlorine Reactions with Dissolved Organic Matter - Assessment of Oxidant-Reactive Moieties by Optical Measurements and the Electron Donating Capacities. *Water Res.* **2018**, *144*, 64–75.
- (50) Rougé, V.; von Gunten, U.; Allard, S. Efficiency of Pre-Oxidation of Natural Organic Matter for the Mitigation of Disinfection Byproducts: Electron Donating Capacity and UV Absorbance as Surrogate Parameters. *Water Res.* **2020**, *187*, 116418.
- (51) Ramseier, M. K.; von Gunten, U. Mechanisms of Phenol Ozonation—Kinetics of Formation of Primary and Secondary Reaction Products. *Ozone: Science & Engineering* **2009**, *31* (3), 201–215.
- (52) Schulze, T.; Meier, R.; Alygizakis, N.; Schymanski, E.; Bach, E.; Li, D. H.; Lauperbe; Raalizadeh; Tanaka, S.; Witting, M. *MassBank/MassBank-Data: Release Version 2021.12*.
- (53) Steenken, S.; Neta, P. Transient Phenoxyl Radicals: Formation and Properties in Aqueous Solutions. In *The Chemistry of Phenols*; John Wiley & Sons, 2003; pp 1107–1152.
- (54) Zhang, K.; Parker, K. M. Halogen Radical Oxidants in Natural and Engineered Aquatic Systems. *Environ. Sci. Technol.* **2018**, *52* (17), 9579–9594.
- (55) Liao, C.-C.; Peddinti, R. K. Masked O-Benzoquinones in Organic Synthesis. *Acc. Chem. Res.* **2002**, *35* (10), 856–866.
- (56) Raghavan, N. V.; Steenken, S. Electrophilic Reaction of the Hydroxyl Radical with Phenol. Determination of the Distribution of Isomeric Dihydroxycyclohexadienyl Radicals. *J. Am. Chem. Soc.* **1980**, *102* (10), 3495–3499.
- (57) Alnaizy, R.; Akgerman, A. Advanced Oxidation of Phenolic Compounds. *Advances in Environmental Research* **2000**, *4* (3), 233–244.
- (58) Zazo, J. A.; Casas, J. A.; Mohedano, A. F.; Gilarranz, M. A.; Rodríguez, J. J. Chemical Pathway and Kinetics of Phenol Oxidation by Fenton's Reagent. *Environ. Sci. Technol.* **2005**, *39* (23), 9295–9302.
- (59) Mvula, E.; von Sonntag, C. Ozonolysis of Phenols in Aqueous Solution. *Org. Biomol. Chem.* **2003**, *1* (10), 1749–1756.
- (60) Prasse, C.; von Gunten, U.; Sedlak, D. L. Chlorination of Phenols Revisited: Unexpected Formation of α,β -Unsaturated C₄-Dicarbonyl Ring Cleavage Products. *Environ. Sci. Technol.* **2020**, *54* (2), 826–834.
- (61) Prasse, C.; Ford, B.; Nomura, D. K.; Sedlak, D. L. Unexpected Transformation of Dissolved Phenols to Toxic Dicarbonyls by Hydroxyl Radicals and UV Light. *Proc. Natl. Acad. Sci. U.S.A.* **2018**, *115* (10), 2311–2316.
- (62) Gazda, M.; Margerum, D. W. Reactions of Monochloramine with Bromine, Tribromide, Hypobromous Acid and Hypobromite: Formation of Bromochloramines. *Inorg. Chem.* **1994**, *33* (1), 118–123.
- (63) Reisz, E.; Fischbacher, A.; Naumov, S.; von Sonntag, C.; Schmidt, T. C. Hydride Transfer: A Dominating Reaction of Ozone with Tertiary Butanol and Formate Ion in Aqueous Solution. *Ozone-Sci. Eng.* **2014**, *36* (6), 532–539.
- (64) Hickel, B.; Sehested, K. Reaction of Hydroxyl Radicals with Ammonia in Liquid Water at Elevated Temperatures. *International Journal of Radiation Applications and Instrumentation. Part C. Radiation Physics and Chemistry* **1992**, *39* (4), 355–357.
- (65) Buffle, M.-O.; Schumacher, J.; Salhi, E.; Jekel, M.; von Gunten, U. Measurement of the Initial Phase of Ozone Decomposition in Water and Wastewater by Means of a Continuous Quench-Flow System: Application to Disinfection and Pharmaceutical Oxidation. *Water Res.* **2006**, *40* (9), 1884–1894.